Jacek REZMER[1], Zbigniew LEONOWICZ[1], Radomir GONO[2]

Wroclaw University of Technology (1), VŠB-Technical University of Ostrava (2)

Analysis of distorted waveforms in power converter systems

Abstract. *We present a method of determining the frequency, developed and based on the Prony model. The method was derived for those cases in which the process contains two dominant harmonics and noise. Additionally, in order to improve the accuracy of the method, median filtering was applied. The presented methods can be useful for practical applications in power systems, like the control systems of frequency converters.*

Streszczenie. *W artykule przedstawiono metodę wyznaczania częstotliwości, opracowaną na podstawie modelu Prony'ego. Metod została opracowana z założeniem, że analizowany proces zawiera dwie harmoniczne i szum. Dodatkowo, w celu poprawy dokładności metody, zastosowano filtrowanie medianowe. Zaprezentowana metoda może być wykorzystana w układach elektroenergetycznych, takich jak układy sterujące przekształtników. (**Analiza przebiegów odkształconych w układach z przekształtnikami**).*

Keywords: Prony model; frequency estimation; waveform distortion; median filter.
Słowa kluczowe: model Prony'ego, estymacja częstotliwości, przebiegi odkształcone , filtr medianowy.

Introduction

Modern solid-state frequency converters used to power among others, the asynchronous motors, are characterized by distorted output voltages waveforms. Due to the control of the rotational speed of the motors, these voltage waveforms may be non-stationary in long intervals of time. Determination of the frequency of fundamental frequency component of converter output voltage is essential for their control systems and for power system apparatus diagnostics and reliability analysis [14]. Non-stationary waveforms causes that the analysis window of digital sampling methods can be very long. When applying short-time Fourier Transform (STFT), accurate results are obtained only when the sampling window has a length equal to the integer multiple of the period of the analyzed component. The length of this period is generally unknown.

Many digital methods of estimation of parameters of the basic component in real time has been developed. The best known use the spectral analysis [1,2,3], Kalman filtering [2,4], parametric methods [11, 12] or artificial neural networks [5]. Most of them have acceptable accuracy when the investigated waveform is slightly distorted. A method based on digital filtering and Prony-model estimation designed for real-time analysis of distorted signal was described in [6, 13].

The paper presents a new method of determining the frequency, developed and based on the Prony model. The method was derived for those cases in which the process contains two dominant harmonics and noise. Additionally, in order to improve the accuracy of the method, median filtering was applied. Extensive simulation studies were carried out for the proposed algorithm. Using the method of band-pass sampling of the signal [7], the reduction of sampling frequency and measurement based on a short sampling window were made possible. The results confirm the accuracy and performance of the method for distorted waveforms in the conditions of dynamic changes in the frequency of the fundamental component.

Description of the method

For *N* given samples of the signal it is assumed that the signal can be approximated by two sinusoidal components

$$\hat{x}_n = A_1 \cos\left(2\pi f_1 n T_p + \psi_1\right) + A_2 \cos\left(2\pi f_2 n T_p + \psi_2\right) \tag{1}$$

where: A_1, A_2 amplitudes of sinusoidal components, f_1, f_2 frequencies of the components , ψ_1, ψ_2 - initial phases of the components T_p -sampling period

Function (1) can be expressed as the sum of complex exponential functions

$$\hat{x}_n = \mathbf{b}_1 \mathbf{z}_1^n + \mathbf{b}_1^* \mathbf{z}_1^{*n} + \mathbf{b}_2 \mathbf{z}_2^n + \mathbf{b}_2^* \mathbf{z}_2^{*n} \tag{2}$$

where:

$$\mathbf{z}_1 = \mathrm{e}^{j2\pi f_1 n T_p}, \quad \mathbf{b}_1 = A_1 e^{j\psi_1} \tag{3}$$

$$\mathbf{z}_2 = \mathrm{e}^{j2\pi f_2 n T_p}, \qquad \mathbf{b}_2 = A_2 e^{j\psi_2} \tag{4}$$

It is assumed that $\mathbf{z}_k$ are roots of a polynomial:

$$a_4 \mathbf{z}^4 + a_3 \mathbf{z}^3 + a_2 \mathbf{z}^2 - a_1 \mathbf{z} + a_0 = 0 \quad \text{or} \tag{5}$$

$$a_0 \left(\mathbf{z} - \mathbf{z}_1\right) \cdot \left(\mathbf{z} - \mathbf{z}_1^*\right) \cdot \left(\mathbf{z} - \mathbf{z}_2\right) \cdot \left(\mathbf{z} - \mathbf{z}_2^*\right) = 0 \tag{6}$$

Because of the relations:

$$2\cos\left(2\pi f_1 T_p\right) = \mathbf{z}_1 + \mathbf{z}_1^* \tag{7}$$

$$2\cos\left(2\pi f_2 T_p\right) = \mathbf{z}_2 + \mathbf{z}_2^* \tag{8}$$

we obtained the relation between f_1, f_2 and coefficients a_0, a_1:

$$2\cos\left(2\pi f_1 T_p\right) = \frac{a_1}{2a_0} - \sqrt{\Delta} \tag{9}$$

$$2\cos\left(2\pi f_2 T_p\right) = \frac{a_1}{2a_0} + \sqrt{\Delta} \tag{10}$$

where $$\Delta = \left(\frac{a_1}{a_0}\right)^2 - \frac{4}{a_0} + 8$$

On the other hand, the coefficients a_0, a_1 can be obtained from signal samples x_n by minimization of mean square error, as follows:

$$E = \sum_{n=1}^{N} \varepsilon_n^{\,2} \quad \text{where} \tag{11}$$

$$\varepsilon_n = x_n - \hat{x}_n \tag{12}$$

This difficult nonlinear estimation problem can be solved by using the Prony method [8, 9], where the approximation error (12) is expressed by the equation:

(13) $$\varepsilon_n = a_0\left(x_{n-2}+x_{n+2}\right)+a_1\left(x_{n-1}+x_{n+1}\right)+a_2 x_n$$

We derive here the minimization of the error (13) with respect to coefficients a_0, a_1

(14) $$\frac{\partial E}{\partial a_0}=\frac{\partial}{\partial a_0}\left\{\sum_{n=2}^{N-2}\left[a_0\left(x_{n-2}+x_{n+2}\right)+a_1\left(x_{n-1}+x_{n+1}\right)+x_n\right]^2\right\}=0$$

(15) $$\frac{\partial E}{\partial a_1}=\frac{\partial}{\partial a_1}\left\{\sum_{n=2}^{N-2}\left[a_0\left(x_{n-2}+x_{n+2}\right)+a_1\left(x_{n-1}+x_{n+1}\right)+x_n\right]^2\right\}=0$$

leads to equations:

(16) $$a_0\sum_{n=2}^{N-2}\left(x_{n-2}+x_{n+2}\right)^2+a_1\sum_{n=2}^{N-2}\left(x_{n-1}+x_{n+1}\right)\left(x_{n-2}+x_{n+2}\right)=-\sum_{n=2}^{N-2}x_n\left(x_{n-2}+x_{n+2}\right)$$

(17) $$a_1\sum_{n=2}^{N-2}\left(x_{n-1}+x_{n+1}\right)^2+a_0\sum_{n=2}^{N-2}\left(x_{n-1}+x_{n+1}\right)\left(x_{n-2}+x_{n+2}\right)=-\sum_{n=2}^{N-2}x_n\left(x_{n-1}+x_{n+1}\right)$$

whose solution is the expression describing the factors a_0, a_1:

(18) $$a_0=\frac{\sum x_n\left(x_{n-1}+x_{n+1}\right)\sum\left(x_{n-1}+x_{n+1}\right)\left(x_{n-2}+x_{n+2}\right)-\sum x_n\left(x_{n-2}+x_{n+2}\right)\sum\left(x_{n-1}+x_{n+1}\right)^2}{\sum\left(x_{n-1}+x_{n+1}\right)^2\sum\left(x_{n-2}+x_{n+2}\right)^2-\left[\sum\left(x_{n-1}+x_{n+1}\right)\left(x_{n-2}+x_{n+2}\right)\right]^2}$$

(19) $$a_1=\frac{\sum x_n\left(x_{n-2}+x_{n+2}\right)\sum\left(x_{n-1}+x_{n+1}\right)\left(x_{n-2}+x_{n+2}\right)-\sum x_n\left(x_{n-1}+x_{n+1}\right)\sum\left(x_{n-2}+x_{n+2}\right)^2}{\sum\left(x_{n-1}+x_{n+1}\right)^2\sum\left(x_{n-2}+x_{n+2}\right)^2-\left[\sum\left(x_{n-1}+x_{n+1}\right)\left(x_{n-2}+x_{n+2}\right)\right]^2}$$

Using (9) and (10) we obtained the frequencies of the signal components f_1, f_2 :

(20) $$f_1=\frac{1}{2\pi T_p}\arccos\left(\frac{a_1}{4a_0}-\frac{\sqrt{\Delta}}{2}\right)$$

(21) $$f_2=\frac{1}{2\pi T_p}\arccos\left(\frac{a_1}{4a_0}+\frac{\sqrt{\Delta}}{2}\right)$$

Signal Sampling

For the discretization of signals containing two major spectral components, one can use band-pass sampling technique, which allows the sampling rate below the Nyquist frequency [7]. Band-pass sampling reduces the requirements for speed and memory capacity of A/D conversion. This technique consists in choosing the sampling frequency such that during the duplication of analog spectrum as a result of sampling, no distortion occurs in the output spectrum of the analyzed component.

Assuming that the frequency f_2 is the carrier frequency component, with high frequency, and the useful signal bandwidth is $2f_1$, the sampling frequency f_p should be chosen from the range obtained by the equation:

(22) $$\frac{2f_2-2f_1}{m}\geq f_p\geq\frac{2f_2+2f_1}{m+1}$$

where m is any even integer number, such that $f_p\geq 4f_1$

Optimal sampling frequency f_{po} lies in the middle of the acceptable frequency band, according to (23):

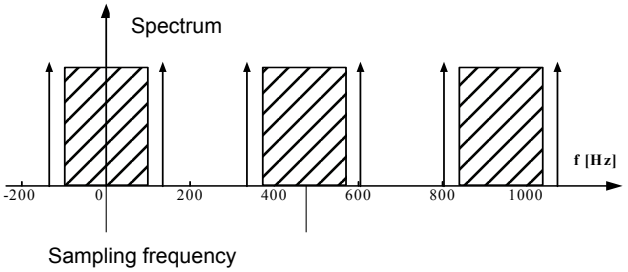

Fig. 1. The use of band-pass sampling method for signals containing two sinusoidal components.

(23) $$f_{po}=\frac{f_2-f_1}{m}+\frac{f_2+f_1}{m+1}$$

Table 1. Band sampling: allowed sampling frequency and the optimum sampling rate for selected parameters; T_p –sampling period [s]

m	f_{pmax}	f_{pmin}	f_{po}	f_p	T_p
46	430,4348	429,7872	430,111	**430**	0,002326
42	471,4286	469,7674	470,598	**470**	0,002128
38	521,0526	517,9487	519,5007	**520**	0,001923
34	582,3529	577,1429	579,7479	**580**	0,001724
28	707,1429	696,5517	701,8473	**700**	0,001429
26	761,5385	748,1481	754,8433	**750**	0,001333
22	900	878,2609	889,1304	**890**	0,001124
18	1100	1063,158	1081,579	**1080**	0,000926

Investigations

In order to examine the performance of the method, a number of simulations were performed for the waveforms consisting of two sinusoidal components and Gaussian noise.

(26)

$$x_n = A_1 \cos\left(2\pi f_1 n T_p + \psi_1\right) + A_2 \cos\left(2\pi f_2 n T_p + \psi_2\right) + e(n)$$

where $e(t)$ is Gaussian random noise with zero mean.

We present here the results of calculations assuming the variable frequency of the fundamental component f_1 changing in the range from 10 Hz to 100 Hz in discrete and continuous way. The high frequency component has a value $f_2 = 10kHz$.

During the simulation we changed the level of noise in the signal, and the parameters of the method, i.e. the width of the analysis window *N* and the width of median filter. Sampling frequency chosen on the basis of relation (23). The allowed sampling frequency bands (f_{pmax} - f_{pmin}) are shown in the Table 1.

The simulation results are presented below. Figure 2 shows a fragment of the test waveform.

Fundamental frequency component changes step-wise in time and subsequently adopts the values, f_1 = 10, 30, 50, 70 and 90 Hz respectively. The frequency of the second component is fixed at f_2 = 10kHz. The signal is sampled according to the technique of band-pass sampling with the frequency f_p = 470 Hz. Amplitudes of the components are respectively $A_1 = 1$, $A_2 = 0.3$. Generated Gaussian random has zero mean value and variance 0.01.

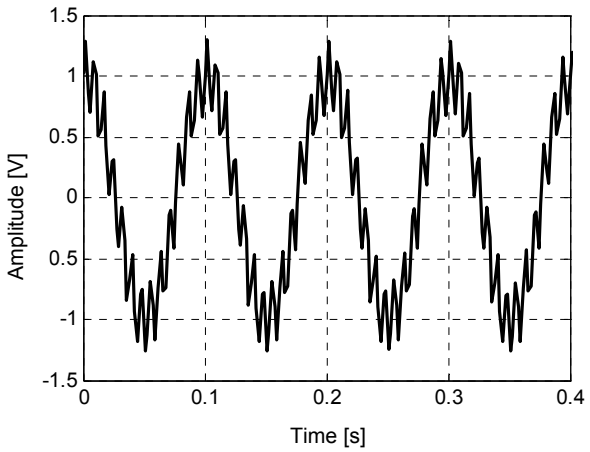

Fig.2. Test voltage waveform. f_1 = 10, 30, 50, 70 and 90 Hz.

Figure 3 presents the results of measuring the frequency of the primary component. The measuring window width is N = 1916 samples and a median filter was applied with a width of $3N$. Subsequent measurements are performed by time shift of the measuring window by one new sample.

Fig. 4 is an enlarged part of Figure 3, shown to demonstrate the accuracy of determining the frequency of the proposed method. In the whole investigated range of frequency changes of the fundamental component the accuracy is comparable The accuracy depends largely on the level of noise and the width of the measuring window.

Figure 5 shows the test process where fundamental frequency component varies linearly over time and takes successively the values of f_1 from 10 to 90 Hz. The frequency of the second component is fixed at f_2 = 10kHz. The signal was sampled according to the technique of band-pass sampling with the frequency f_p = 470 Hz.

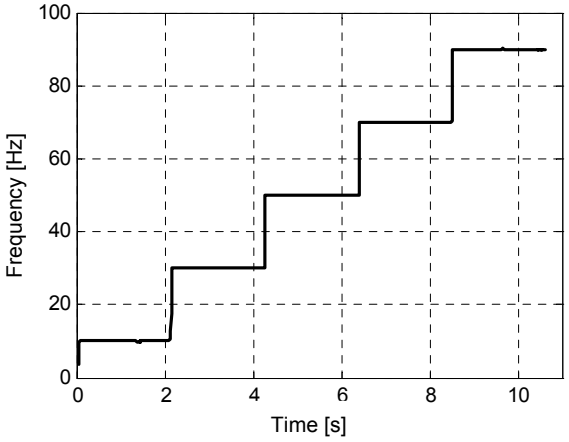

Fig.3. The results of measuring the frequency of fundamental component, N = 16, filter length- $3N$.

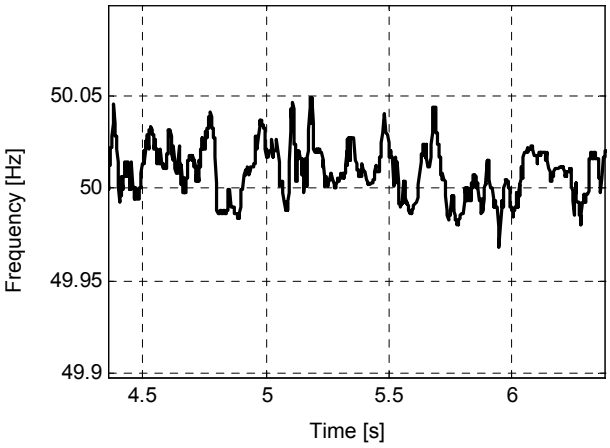

Fig.4. Results of the frequency measurement of the fundamental component - enlarged fragment of Figure 3, N = 16, filter length-$3N$.

Amplitudes of components are, respectively, A_1 = 1, A_2 = 0.3. Generated Gaussian random noise has a mean value of zero and variance 0.01.

Figure 6 presents the results of measuring the frequency of fundamental component which varies linearly in time. The measuring window width applied *N* = 16 samples and a median filter with a width of 3*N*.

Fig. 7 is an enlarged part of the Fig. 6 shown to demonstrate the accuracy of determining the frequency. In the whole investigated range of frequency changes of the component the accuracy is similar.

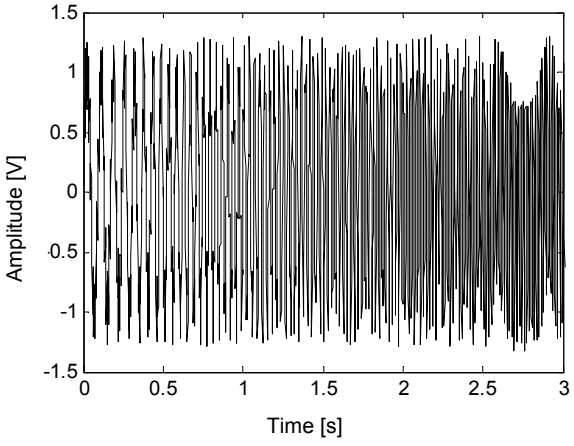

Fig.5. The test voltage process, f_1 = 10-90 Hz varies linearly in time, f_2 = 10kHz, f_p = 470 Hz

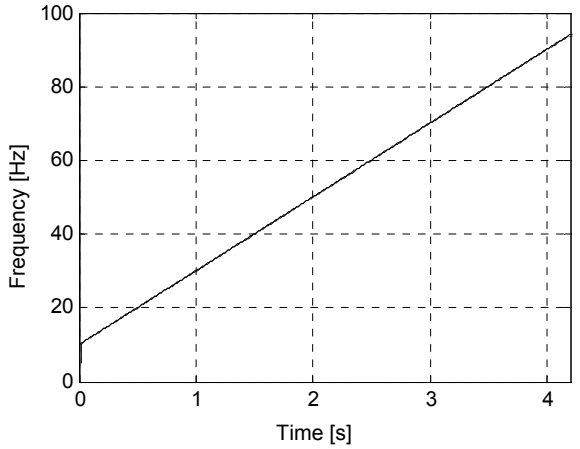

Fig.6. The results of measuring the frequency of fundamental component of the test process of Figure 5, N = 16, filter length-$3N$.

The frequency determination process, as shown in above examples, because of the band-pass sampling method, allows only to correctly calculate the fundamental frequency component, whose knowledge is essential for the control system. In the case, however, when the sampling frequency is greater than Nyquist frequency of $2f_2$, the method correctly finds the two components of the signal.

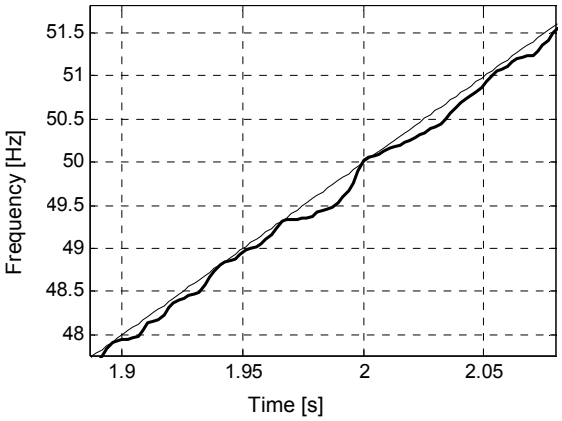

Fig.7. Results of the frequency measurement of fundamental component - enlarged fragment of Figure 6, N = 16, filter length $3N$.

Conclusions

The paper presents a method of determining the frequency of time-varying distorted waveform, such as voltage waveforms encountered in inverter power drives.

Conducted extensive studies of the proposed method, confirm its correctness and indicate the field of possible applications.

Distorted signals were investigated, consisting of two dominant harmonics. The signal also contained noise and model of signal distortion typical for digital signal processing channel. As a result of these studies we found that with proper choice of parameters of the method, it allows the precise calculation of the frequency of fundamental component.

This work was supported by the Czech Science Foundation (No. GA ČR 102/09/1842).

REFERENCES

[1] Phadke A.G., Thorp J.S., Adamiak M.G., A new measurement technique for tracking voltage phasor, local frequency and rate of change frequency, *IEEE Trans. on Power Apparatus and Systems*, vol. PAS-102 (1983), 1025-1038

[2] Łobos T., Nonrecursive method for real-time determination of basis waveforms of voltages and currents, *IEE Proceedings Gener. Transm. and Distrib*, vol. 136 (1989), no 6, 347-351

[3] Eichhorn K.F., Łobos T., Recursive real-time calculation of basic waveform of signals, IEE Proceedings Gener. Transm. and Distrib, vol. 138 (1991), no 6, 469-470

[4] Girgis A.A., Grown R.G., Application of Kalman filtering in computer relaying. *IEEE Trans. on Power Apparatus and Systems*, vol. PAS-100 (1981), 3387-3395

[5] Cichocki A., Łobos T., Artificial neural networks for real-time estimation of basic waveforms of voltages and currents. *IEEE Trans. on Power Systems*, vol. 9 (1994), 612-618

[6] Łobos T., Rezmer J., Real-time determination of power systems frequency. *IEEE Trans. on Instrumentation and Measurement*, vol. 46 (1997), no 4, 877-881

[7] Lyons R.G., *Understanding Digital Signal Processing*, Prentice-Hall, (1999)

[8] Kay, S.M., Modern Spectral Estimation: Theory and Application. Prentice-Hall, Englewood Cliffs, (1988)

[9] Osborne, M.R. Smyth G.J. (1995) A modified Prony Algorithm for exponential function fitting. *SIAM J. Sci. Statist. Comput*. 16 (1995), 119-138

[10] Łobos T.; Rezmer J., Schegner P., Parameter Estimation of Distorted Signals Using Prony Method. *2003 IEEE Bologna PowerTech Proceedings* , Bologna, Italy, June 23-26, (2003)

[11] Łobos T.; Leonowicz Z., Piotrowicz J., Detection of the Fundamental Harmonic of Distorted Signals using Min-Norm Method, *10. International Symposium on Theoretical Electrical Engineering, September 6-9, Magdeburg (Germany)*, (1999)

[12] Łobos T., Leonowicz Z., Rezmer J., Schegner P., High-resolution Spectrum Estimation Methods for Signal Analysis in Power Systems, *IEEE Trans. on Instr. Meas*., vol. 55 (2006), No. 1, 219-225

[13] Łobos T., Rezmer J., Detection of the frequency of Distorted Signals in Converter Systems, „Wyznaczanie częstotliwości zniekształconych sygnałów w układach przekształtnikowych (in Polish)". *Wiadomości Elektrotechniczne*. 71(7/8) (2003), 312-315

[14] Rusek S., Gono R., Kratky M., Dvorsky J., A framework for an analysis of failure data in electrical power networks, *Proc. IASTED International Conference on Power, Energy*, and Applications Sep 11-13, (2006), Gaborone, Botswana, 45-46.

***Authors**: dr inż. Jacek Rezmer, Politechnika Wrocławska, Instytut Podstaw Elektrotechniki i Elektrotechnologii, Wyb. Wyspiańskiego 27, 50-370 Wrocław, Poland, E-mail: jacek.rezmer@pwr.wroc.pl; dr. inż. Zbigniew Leonowicz, Politechnika Wrocławska, Instytut Podstaw Elektrotechniki i Elektrotechnologii, Wyb. Wyspiańskiego 27, 50-370 Wrocław, Poland, E-mail: leonowicz@ieee.org, Doc. Ing. Radomir Gono, VSB - Technical University of Ostrava, Faculty of Electrical Engineering and Computer Science, Department of Electrical Power Engineering, 17. listopadu 15, 708 33 Ostrava – Poruba, Czech Republic, E-mail: radomir.gono@vsb.cz*